ADVANCES IN ATMOSPHERIC SCIENCES, VOL. 34, MARCH 2017, 321–334

• **Original Paper** •

The Long-term Variation of Extreme Heavy Precipitation and Its Link to Urbanization Effects in Shanghai during 1916–2014

Ping LIANG*[1] and Yihui DING[2]

[1]*Shanghai Climate Center, Shanghai* 200030, *China*

[2]*National Climate Center, Beijing* 100081, *China*

(Received 23 April 2016; revised 20 September 2016; accepted 26 September 2016)

ABSTRACT

Using the hourly precipitation records of meteorological stations in Shanghai, covering a period of almost a century (1916–2014), the long-term variation of extreme heavy precipitation in Shanghai on multiple spatial and temporal scales is analyzed, and the effects of urbanization on hourly rainstorms studied. Results show that: (1) Over the last century, extreme hourly precipitation events enhanced significantly. During the recent urbanization period from 1981 to 2014, the frequency of heavy precipitation increased significantly, with a distinct localized and abrupt characteristic. (2) The spatial distribution of long-term trends for the occurrence frequency and total precipitation intensity of hourly heavy precipitation in Shanghai shows a distinct urban rain-island feature; namely, heavy precipitation was increasingly focused in urban and suburban areas. Attribution analysis shows that urbanization in Shanghai contributed greatly to the increase in both frequency and intensity of heavy rainfall events in the city, thus leading to an increasing total precipitation amount of heavy rainfall events. In addition, the diurnal variation of rainfall intensity also shows distinctive urban–rural differences, especially during late afternoon and early nighttime in the city area. (3) Regional warming, with subsequent enhancement of water vapor content, convergence of moisture flux and atmospheric instability, provided favorable physical backgrounds for the formation of extreme precipitation. This accounts for the consistent increase in hourly heavy precipitation over the whole Shanghai area during recent times.

Key words: hourly precipitation, long-term trend, urbanization, extreme events

Citation: Liang, P., and Y. H. Ding, 2017: The long-term variation of extreme heavy precipitation and its link to urbanization effects in Shanghai during 1916–2014. *Adv. Atmos. Sci.*, **34**(3), 321–334, doi: 10.1007/s00376-016-6120-0.

1. Introduction

From the first IPCC assessment report (IPCC, 1990) to the fifth (AR5) (IPCC, 2013), the major conclusions show unequivocally that the global climate is warming. Land-surface warming increases the atmospheric water vapor content by accelerating surface evaporation. Meanwhile, the water-holding capacity of the atmosphere is enhanced by the increase in temperature, which increases the efficiency of precipitation formation (Trenberth, 2005). The intensity of extreme precipitation is likely to be enhanced in most land areas over the midlatitudes and humid tropics (IPCC, 2013). Trends of regional annual precipitation are primarily driven by changes in the top 30% of heavy precipitation events, which are controlled by changes in precipitable water in response to global warming (Liu et al., 2016). As indicated in IPCC AR5, global warming since the mid-20th century may be mainly attributable to anthropogenic influences (IPCC, 2014), and the climate warming associated with human activity is conducive to increased precipitation (Ding et al., 2007; 2009; Piao et al., 2010). However, the impacts of urbanization on rainfall vary among different cities with different intensities of human activity (Gao et al., 2004). In China, Shanghai (Zhou and Yang, 2001; Mu et al., 2008; Liang et al., 2013), Nanjing (Zhou et al., 2003) and Tianjin (Yu et al., 2008) show rain-island characteristics, while cities including Beijing (Sun and Shu, 2007; Wang et al., 2009) and Chengdu (Hao et al., 2007) exhibit dry-island features. Liang et al. (2013) suggested that the spatial distribution of rainstorm frequency in Shanghai under rapid urbanization, as well as its trend, has a more distinct urban rain-island feature than under slow urbanization. In Beijing, the impact of urbanization on precipitation is primarily reflective of the dry-island effect, but the frequency of torrential rain above 100 mm d^{-1} (Hu, 2015), as well as the strength of low temperature sleet events (Han et al., 2014), is greatly influenced by the urban rain-island effect. Although many studies on the influences of urbanization on rainfall have been conducted, the impacts on short-duration or hourly heavy rainfall remain unclear.

For China as a whole, the frequency of extreme heavy precipitation events has significantly increased in the long-term (1957–2003; Zhai et al., 2007). However, influenced by synoptic systems and terrain, the characteristics of tempo-

* Corresponding author: Ping LIANG
Email: liangping1107@163.com

ral or spatial distributions of heavy rainfall vary among different areas (Cai et al., 2007; Lin and Yang, 2014). For instance, the frequency and intensity of drought events over the Haihe River basin have increased (Liu et al., 2010); whereas, extreme precipitation events over most areas of the middle and lower reaches of the Yangtze River and South China show an obvious upward trend (Chen et al., 2009). In general, recent studies on precipitation and extreme precipitation events in China have mainly been based on daily rainfall data, which might mask the features of short-duration heavy rainfall events (Li et al., 2013). Instead, greater objectivity could perhaps be achieved by investigating the characteristics of rainstorm events and their related mechanisms through the use of hourly data. Previous research on hourly precipitation in China has focused mainly on the diurnal variation of precipitation (Yin et al., 2011b; Zhang and Zhai, 2011; Huang et al., 2012; Li et al., 2013; Yu et al., 2014; Han et al., 2014), revealing that the diurnal variation of precipitation and the long-term trend of low-temperature sleet events are related to increased surface temperature and difference in topography. Other studies that applied hourly data analyzed the relationships between the frequency of heavy rainfall events and large-scale air–sea factors, including the Pacific Decadal Oscillation, ENSO and the North Atlantic Oscillation (Grimm and Tedeschi, 2009; Vicente-Serrano et al., 2009; Pattanaik and Rajeevan, 2010; Fu et al., 2010; Boschat et al., 2015). But what are the impacts of climate change on hourly heavy rainfall events? And what contributions are made by urbanization? These problems are still not clear.

In order to further understand the association between extreme precipitation and climate change, this paper, by taking Shanghai as an example, investigates the spatiotemporal distribution of extreme precipitation over a long-term period of almost a century (1916–2014), based on quality-controlled hourly precipitation data. The effect of urbanization on the long-term trends of extreme precipitation is then also evaluated. The hope is that the results will benefit improvements in numerical modeling (Huang et al., 2009) and urban disaster prevention and mitigation.

Following this introduction, section 2 describes the study area (including Shanghai's urbanization history), data and statistical methods used in this work. In section 3, the variability of hourly heavy precipitation events during the last century in Shanghai is analyzed on multiple scales. Section 4 presents the temporal evolution of the spatial distribution of heavy precipitation. In section 5, the influence of urbanization on the spatial distribution of heavy rainfall, as well as its variation tendency, are investigated. Section 6 discusses the possible effects of climate change on the variation trends of heavy precipitation in Shanghai. And finally, a summary of the study's key findings is provided in section 7.

2. Study area, data and methods

2.1. *Study area and urbanization history*

Located in the alluvial plain of the Yangtze River Delta, Shanghai is a coastal megacity with an average altitude of 4 m. Shanghai sits on the south edge of the mouth of the Yangtze River. The municipality borders the provinces of Jiangsu and Zhejiang to the north, south and west, and is bounded to the east by the East China Sea and to the south by Hangzhou Bay (Fig. 1a). As a global financial center, Shanghai has experienced rapid urbanization and economic development. Based on variations of urban factors reflected by population density and paved road area (Fig. 1b; data from Shanghai Bureau of Statistics, http://www.stats-sh.gov.cn/index.html), it can be clearly seen that, compared with the relatively slow urbanization period before the 1980s, both the urban population and paved road areas in Shanghai have grown dramatically over the past 30 years—especially since the 1990s, when economic reforms were introduced in Shanghai. By 2014, Shanghai's population density (3826 km^{-2}) and paved road area (279.18×10^6 m^2) had grown considerably compared with 1960 (1787 km^{-2} and 7.5×10^6 m^2, respectively).

2.2. *Data*

The annual records of maximum hourly precipitation from 11 meteorological stations in Shanghai for the period 1916–2014 are used in this paper. The locations of these 11 stations are shown in Fig. 1a. The data were collected and quality-controlled by the Shanghai Meteorological Information Center (SMIC) of the Shanghai Meteorological Bureau. Among them, the station at Xujiahui has a long record (since 1916), while Jiading, Pudong, Fengxian, Qingpu and Jinshan have been in operation since 1959. Data from Nanhui, Baoshan and Minhang began to be collected in 1962, 1965 and 1966, respectively, while Songjiang and Chongming stations have been recording data since 1981. Precipitation amounts were automatically recorded by autographic rain gauges, including tilting siphons and tipping-bucket rain gauges. All of the rain gauges have been positioned at 0.7 m above the ground since their respective rainfall records began. The maximum hourly precipitation was determined through minute-by-minute observations, on an annual basis, by the autographic rain gauges and archived by SMIC after quality control. Following Wijngaard et al. (2003), the homogeneity of the data during the study period was investigated through combined use of the Standard Normal Homogeneity Test (Alexandersson, 1986), the Buishand Range Test (Buishand, 1982), and the Pettitt Test (Pettitt, 1979). The results revealed a suspicious inhomogeneity at Xujiahui station in 1976. In fact, there was no station migration or alteration of the observation environment at this time, but an extraordinary storm with disastrous flooding consequences for the whole of Shanghai did occur on the afternoon of 7 September 1976 (Xu, 2006). Therefore, this suspicious inhomogeneous point in the data caused by this weather event was removed from the precipitation dataset used in this paper.

The hourly precipitation data from the same 11 meteorological stations in Shanghai, but for the period 1981–2014, from the National Meteorological Information Center of the China Meteorological Administration (CMA), are also applied in this paper. This dataset were subjected to stringent

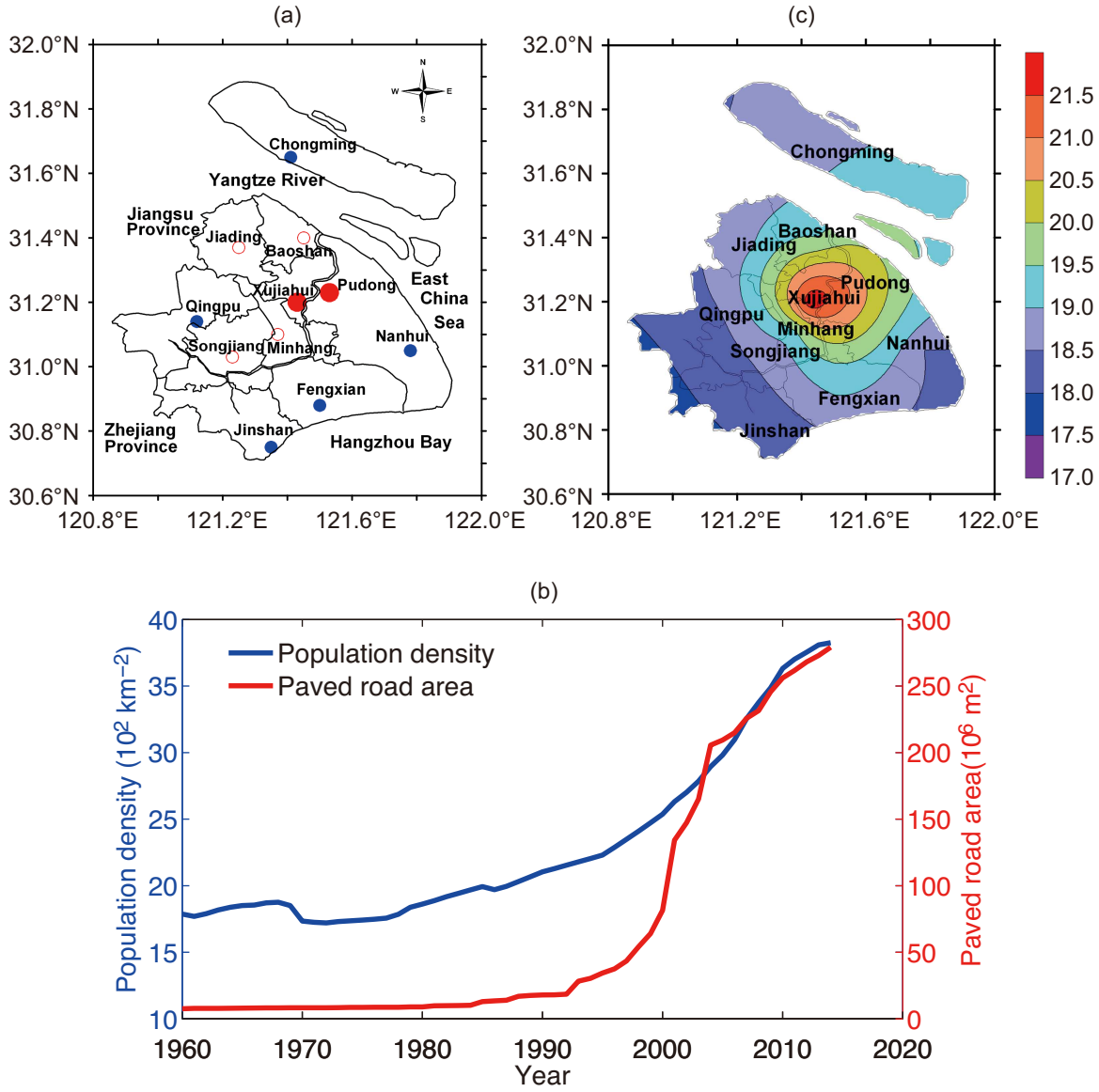

Fig. 1. (a) Locations of 11 meteorological stations in Shanghai (filled red circles: urban stations; filled blue circles: rural stations; open red circles: suburban stations). (b) Evolution of urbanization reflected by population density and paved road area. (c) Spatial distribution of thresholds of hourly heavy rainfall (units: mm).

quality-control, and have been widely used in many previous studies (e.g., Yin et al., 2011b; Zhang and Zhai, 2011; Li et al., 2013; Yu et al., 2014). The measurement instruments and background were the same as for the annual maximum data mentioned above.

NCEP–NCAR daily reanalysis (NNR) data (Kalnay et al., 1996), including temperature and relative humidity fields, during 1981–2014, are used to calculate the long-term change in atmospheric instability and water vapor.

2.3. *Methods*

Following the urban classification criteria of Zhou and Shi (1995), the population densities in 2008 of the 11 districts where the meteorological stations are located were used to classify the stations into three types. Specifically, Xujiahui and Pudong, with their population densities being above 3000 km^{-2}, were classified as "urban" stations; Chongming, Nanhui, Jinshan, Qingpu and Fengxian, at less than 1500 km^{-2}, were classified as "rural" stations; and the remaining stations, including Minhang, Baoshan, Jiading and Songjiang, were classified as "suburban" stations. The reason for using the population statistics in 2008 to classify the stations was that Nanhui district was merged into Pudong district in 2009, which meant there were no population records for the original Nanhui district thereafter, and a dramatic decrease in the population density of the now larger Pudong district. As shown in Fig. 1a, the rural stations, indicated by the blue spots, are located in the periphery of Shanghai city; the urban stations, represented by red spots, sit on the central part of the city; and the suburban stations are situated between the rural and urban stations.

The hourly records of the 11 meteorological stations in

Shanghai since 1981 are used to examine the variations of hourly precipitation events during the period of rapid urbanization. Specifically, the threshold for heavy rainfall is classified by the 99.9th percentile of hourly rainfall in the summer half of the year (April to September) during this period (1981–2014). The percentile method is a nonparametric method applicable to data with all kinds of distributions, and is widely used for thresholds relating to extreme rainfall. The thresholds of the 11 stations range from 18.1 to 21.9 mm, which is close to the threshold for short-duration heavy precipitation (i.e., 20 mm h^{-1}) currently in operation under the regulations of the CMA. As shown in Fig. 1c, heavy rainfall events concentrated at city stations (Xuhui, Pudong) are usually stronger than those over the suburbs (Baoshan, Minhang, Jiading, Songjiang) and coastal stations (Fengxian, Nanhui and Chongming), with coastal station rainfall being stronger than over the suburbs.

A linear tendency estimation method (Wei, 2007) is used in this paper to calculate long-term trends; and following Meals et al. (2011), Mann–Kendall nonparametric tests (Mann, 1945; Kendall, 1975) are applied to detect the significance of trends. To reduce uncertainties brought about by the linear tendency estimation, Ensemble Empirical Mode Decomposition (EEMD; Wu and Huang, 2005, 2009)—a method for processing nonlinear and non-stationary series—is also employed, for further comparative analysis of the long-term trends of heavy precipitation. EEMD is the result of improvements made to its predecessor, EMD (Empirical Mode Decomposition; Huang et al., 1998), and involves four main steps: (1) Add a noise series to the target data; (2) Decompose the data with the added noise into Intrinsic Mode Functions (IMFs); (3) Repeat (1) and (2) again and again, but with different noise series each time; (4) Obtain the ensemble means of the corresponding IMFs of the decompositions as the final result. This approach can solve the mode mixing problem of EMD and make the mean IMFs stay within the natural filter period windows. In addition, we use a Gaussian filter (Barnes, 1973) to obtain the decadal components of time series. EOF analysis (Lorenz, 1956) is also used, to analyze the spatial distribution of the long-term evolution of heavy rainfall events.

In order to analyze the atmospheric stability, the K index is applied (Zhang et al., 2007), defined as

$$K = (T_{850} - T_{500}) + T_{d850} - (T_{700} - T_{d700}) \quad (1)$$

where $(T_{850} - T_{500})$ indicates the temperature contrast between the lower and middle level, i.e., the rate of vertical temperature decline; T_{d850} denotes the 850-hPa dew-point temperature, characterizing the moisture content at the low level; and $(T_{700} - T_{d700})$ expresses the difference between the temperature and dew-point at 700 hPa, which denotes the low-level water vapor saturation. The K index is a comprehensive index able to reflect the atmospheric potential energy by characterizing the humidity and saturation degree of the lower troposphere. At the same time, it can also reflect the warmth of the lower layers. Both are important for describing the atmospheric instability. Therefore, it is widely used in the forecasting and analysis of severe convective weather, especially heavy rainfall events (Zhang et al., 2007). As described in Wang et al. (2012), NNR data can be used to calculate the K index, because of the close correlation between the K index acquired from operational sounding observations and that from NNR data. Therefore, in this paper, the NNR data are employed to analyze the trends of unstable atmospheric stratification for three layers in association with heavy precipitation. In addition, NNR data are commonly used for calculating the water vapor transport flux due to the stratification of the water vapor balance equation. Accordingly, the NNR data are also used in this study to calculate the trends of water vapor transport.

3. Multiscale variability of extreme precipitation events

3.1. *Long-term annual variation of hourly maximum precipitation*

From the long-term annual variation of hourly maximum precipitation at Xujiahui shown in Fig. 2a, we can see that the hourly precipitation maximum has increased significantly (>95% confidence), with a trend of 2.72 mm h^{-1} (10 yr)$^{-1}$. Furthermore, trend is especially significant [6.60 mm h^{-1} (10 yr)$^{-1}$] during the rapid urbanization period (1981–2014). Similarly, the annual hourly maximum averaged in Shanghai also shows a significant (>99.9% confidence) increasing trend (Fig. 2b), with a rate of 6.2 mm h^{-1} (10 yr)$^{-1}$, for nearly half a century (1965–2014). The average maximum during the latest 10 years (2005–14) rose by half as much compared with that (57 mm h^{-1}) during the 10 years from 1965 to 1974. In addition, from the changes in the distribution parameters of the annual maximum at Xujiahui during every 30 years with a 10-year sliding window (figure omitted), all of the distribution parameters, including median, skewness and kurtosis, as well as the shape parameter fitted by the General Extreme Value distribution (Coles et al., 2001), are largest during the latest 30 years (1986–2014), meaning that both the strength and probability of extreme heavy precipitation enhanced during the rapid urbanization period.

Figure 2c shows the distribution of the 99.9th percentile for the annual maximum of hourly precipitation in Shanghai since 1916. It gradually decreases outward from Xujiahui and Pudong stations in downtown Shanghai, suggesting a distinct urban rain-island feature. Those stations located downstream of the prevailing southeasterly wind during summer (Jiading, Baoshan, Qingpu) also experienced relatively heavy rainstorms; whereas, extreme heavy precipitation at the coastal sites (e.g., Nanhui, Jinshan) was weaker than at the inland and city sites.

3.2. *Changes in hourly heavy precipitation during the rapid urbanization period*

As shown in Fig. 3a, during the rapid urbanization stage, the frequency of hourly heavy precipitation exhibits an upward long-term trend at a rate of 3.2 yr^{-1}. Furthermore, the

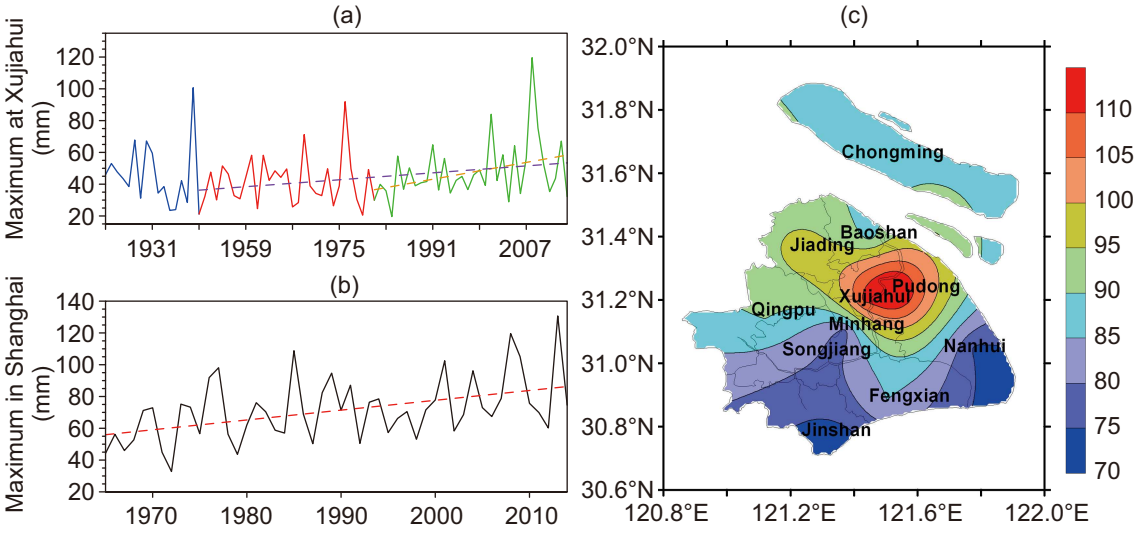

Fig. 2. Annual evolution of maximum hourly precipitation (units: mm): (a) records at Xujiahui, covering almost 100 years; (b) records for the whole of Shanghai, covering nearly 50 years; (c) spatial distribution of the 99.9th percentile of annual hourly precipitation maximum in Shanghai since 1916.

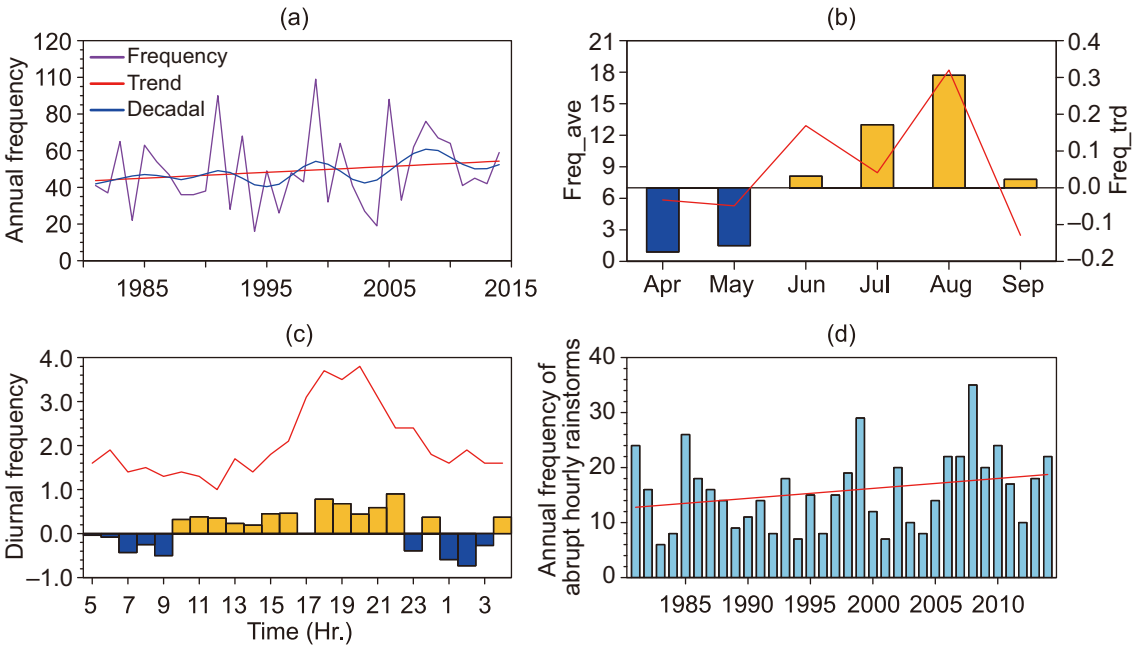

Fig. 3. Variation in the frequency of hourly rainstorms in Shanghai during the rapid urbanization period (units of trend: yr^{-1}): (a) interannual variation (red/blue line denotes trend/decadal component); (b) monthly variation (represented by histogram; red line denotes monthly trend); (c) diurnal variation (represented by red line; histogram denotes hourly trend); (d) annual frequency of abrupt hourly rainstorms (red line is the trend line).

case is similar for its decadal component after the interannual variability has been filtered, especially since the late 1990s. The average annual frequency during 1998–2014 is 53 yr^{-1} over the whole Shanghai area, which is 8 yr^{-1} more than that during 1981–97. However, there is little change in the total rainfall amount during April to September before and after 1997, which suggests that hourly heavy precipitation occurred more frequently after the late 1990s.

The monthly frequency of hourly heavy precipitation shows a unimodal type distribution (Fig. 3b). The frequency peak occurs in July and August (highest in August), accounting for 63% of the summer half of the year. The occurrence of heavy precipitation during April–May is about 2 yr^{-1}, accounting for only 5% of the summer half of the year. From the long-term change in the monthly frequencies of hourly heavy precipitation (Fig. 3b), the occurrence probability in August increases significantly (>90% confidence), with a rate of 3.2 $(10\ yr)^{-1}$. In addition, the probability in June also

shows a positive trend [1.7 (10 yr)$^{-1}$]. Conversely, the probability in September shows a significant negative tendency [−1.3 (10 yr)$^{-1}$], while there is no obvious trend for July.

The diurnal variation of the frequency of hourly heavy rainfall events (Fig. 3c) also shows a unimodal-type distribution, with the peak reaching 3.4 yr^{-1} at 1700–2100 local standard time (LST). However, heavy rainfall occurs relatively less frequently in the morning (0500–1200 LST). There is a consistent increasing trend for heavy rainfall events during daytime (1000–2200 LST). Therefore, the trend [0.7 (10 yr)$^{-1}$] at peak time (1800–2200 LST) is the most distinctive.

Due to the considerable influence of the pattern of intense rainfall on flood prevention and drainage, the temporal evolution of intense precipitation is further examined according to a classification of temporal evolution patterns (Table 1). On average, abrupt events account for half of all types, while the growing or persistent types contribute 28.1% and 21.9%, respectively. As shown in Fig. 3d, during modern times, abrupt heavy precipitation have dramatically increased, with a trend of 1.8 (10 yr)$^{-1}$ (90% confidence level); whereas, the growing type events show a downward trend [−0.75 (10 yr)$^{-1}$], and the trend for persistent type events is indistinct. In other words, hourly heavy precipitation has become more abrupt in Shanghai since 1981.

4. Evolution of the spatial distribution of heavy precipitation events

The results presented in section 3 demonstrate that hourly heavy rainfall in Shanghai occurred more frequently during the rapid urbanization period. Next, we discuss the evolution of spatial differences in heavy rainfall in Shanghai, and the link with urbanization.

4.1. *Spatial differences in the variation trends of heavy precipitation in Shanghai*

As shown in Fig. 4a, the spatial distribution of the trends of hourly heavy precipitation frequency is clearly influenced by urbanization. Urban (Xujiahui and Pudong) and suburban (Minhang and Jiading) stations show distinctive increasing trends, reaching 0.5–0.7 (10 yr)$^{-1}$, while rural sites show weak upward trends or downward trends. According to the results presented in section 3, the annual frequency over the whole Shanghai increased during the rapid urbanization period, which means heavy rainfall events were focused more in urban and suburban areas.

Table 1. Classification of temporal evolution types of heavy rainfall events.

Temporal evolution type	Precipitation conditions during the 3 h before the heavy rainfall event (P_{-1}, P_{-2}, P_{-3}, respectively; P denoting precipitation)
Abrupt type	$P_{-1} < 0.5$ mm, $P_{-2} < 0.5$ mm and $P_{-3} < 0.5$ mm
Growth type	$P_{-2} > P_{-1}$ or $P_{-3} > P_{-1}$ and one of P_{-1}, P_{-2} or P_{-3} larger than 0.5 mm but less than the threshold of heavy precipitation events
Continuous type	One of P_{-1}, P_{-2} or P_{-3} larger than the threshold of heavy rainfall events

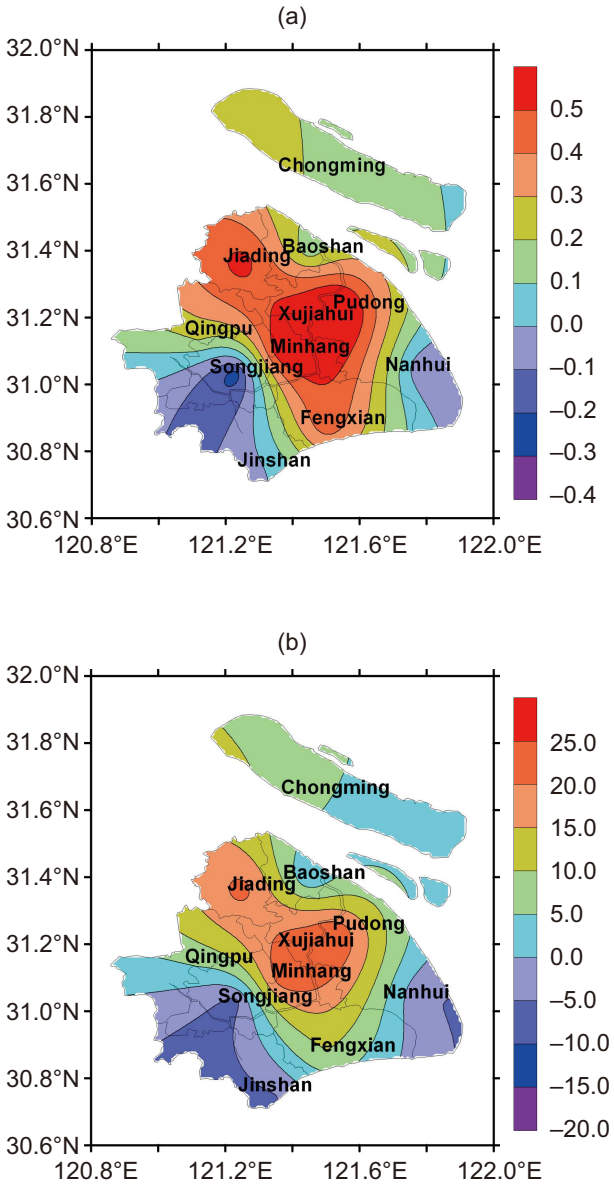

Fig. 4. Spatial distribution of the trend of the (a) frequency [units: (10 yr)$^{-1}$] and (b) total precipitation amount [units: mm (10 yr)$^{-1}$] of hourly rainstorms.

The urban rain-island feature is also reflected in the trends of heavy rainfall event total precipitation amounts. As shown in Fig. 4b, frequencies over central urban (Pudong and Xujiahui) and nearby suburban (Minhang and Jiading) sites increased dramatically, with rates of 21.7–25 mm (10 yr)$^{-1}$. In addition, the trends for Pudong and Jiading exceed the 0.10 confidence test, whereas the trends at rural stations are not clear and, in some cases, even show a slight reduction. Therefore, urbanization may contribute to the spatial differences of the evolution trends of both frequency and total rainfall amount for heavy rainfall events in Shanghai.

4.2. *Evolution of spatial types of heavy rainfall events*

Further calculations are made with respect to spatial distribution types of hourly heavy rainfall events in Shanghai, according to the information given in Table 2. As depicted in Fig. 5, on average, local heavy rainfall occurs most frequently (~25 yr^{-1}), accounting for 74.5% of all types. Meanwhile, the small range type accounts for 22.3% (~8 yr^{-1}), and regional and large-scale events are least probable (3.2%). These results suggest that hourly heavy precipitation events possess obvious local or small-scale features. When it comes to long-term change, both local- and small-scale events show obvious increasing trends, especially the local type, reaching 1.5 (10 yr)$^{-1}$. The largest rise in frequency of local heavy rainfall is located in the central city area and suburbs to the south, exhibiting a fan-shaped distribution from the former to the latter along the Huangpu River (figure omitted). This pattern of more local heavy rainfall over the central city area and southern suburbs may be associated with wind convergence brought by the urban heat island effect and sea–land breeze circulation, respectively (Hu and Li, 2010). Further calculations show local and small-scale precipitation events in June and August increase significantly, with rates at 1.0 (10 yr)$^{-1}$ and 1.4 (10 yr)$^{-1}$, reaching the 95% and 99% confidence level, respectively. This is consistent with the increasing trend for the annual frequency of heavy rainfall events during June and August, mentioned in section 3.2.

5. Influences of urbanization on the long-term variation of heavy precipitation

5.1. *Impacts on spatial distribution*

In order to further identify whether there are different regional regimes of climate variability in heavy precipitation events in association with the urban–rural difference in Shanghai, EOF analysis is applied to the anomaly time series of frequencies and total amounts of heavy precipitation events in Shanghai during the rapid urbanization period (1981–2014). The first EOF mode (figures omitted) for both the frequency and total rainfall amount of heavy precipitation explains about 48% of the total variance, exhibiting coherent increasing phases over the whole of Shanghai. This may be connected with the regional consistency of warming in Shanghai. The specific reasons will be discussed in section 6; however, here, we focus on the urban–rural differences associated with urbanization, which can be distinctively found in the second EOF modes. From Fig. 6a, the second eigenvector (EOF2) by EOF on frequencies of heavy precipitation events, with a variance contribution rate of 12.4%, shows a reverse distribution type from south to north. Because urban and suburban stations are locate in north or central Shanghai, respectively, the spatial distribution of EOF2 might reflect the variation of urban–rural differences. As shown in Fig. 6b, the principal component of EOF2 tends to reduce. In other words, in modern times, since 1981, the frequencies of heavy precipitation events over urban and nearby suburban areas have enhanced more than in rural areas over south Shanghai. Therefore, urbanization plays an important role in the spatially inhomogeneous distribution of the frequency of heavy precipitation. The second eigenvector (EOF2) of total heavy precipitation amounts, with a variance contribution rate of 12.1% (Fig. 6c), exhibits a more obvious rain-island feature in the central city area. Furthermore, its principal component (Fig. 6d) has also significantly increased, at the 95% confidence level. Therefore, urbanization makes a more distinctive contribution to the strengthening of heavy rainfall than that of the frequency of heavy rainfall. This result matches well with the study of Tan et al. (2015), based on surface AWS monitoring records, which also showed the presence of an urban rain island. It is worth mentioning that, for the first EOF modes with consistent phases, the fact that larger amplitudes were located at urban stations suggests that warming as a result of urbanization also, to some extent, exerted effects on the evolution of the first EOF spatial distribution of heavy precipitation in Shanghai.

Table 2. Classification of spatial distribution types of heavy rainfall events.

Spatial distribution type	Station coverage percentage
Local	< 10%
Small-scale	⩾ 10% and < 33.3%
Regional	⩾ 33.3% and < 50%
Large-scale	⩾ 50%

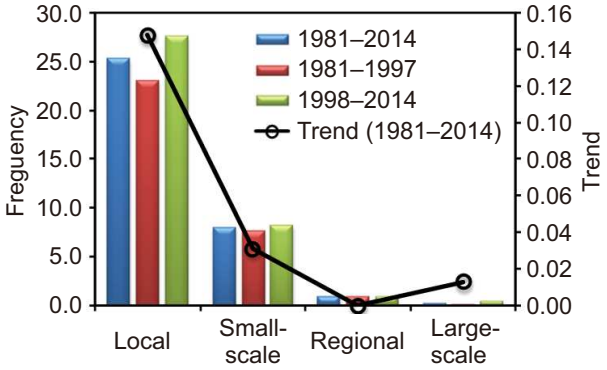

Fig. 5. Average frequencies for different timespans (bars) and trend (curve) of heavy rainfall events belonging to different spatial distribution types (units: yr^{-1}).

5.2. *Impacts on long-term trends*

As described in section 2.3, based on population density in Shanghai, Xujiahui and Pudong were selected as urban sites, while Chongming, Nanhui, Jinshan, Qingpu and Fengxian were selected as rural stations. Using this classification, i.e., through urban–rural comparison, the effects of urbanization on the long-term change in heavy rainfall can be investigated. The long-term trends for total rainfall amount, frequency and strength of heavy precipitation at the above two types of observatories (i.e., urban and rural) exhibit distinct differences, and these differences are consistent with the urban-island effects described in section 5.1. To quantify

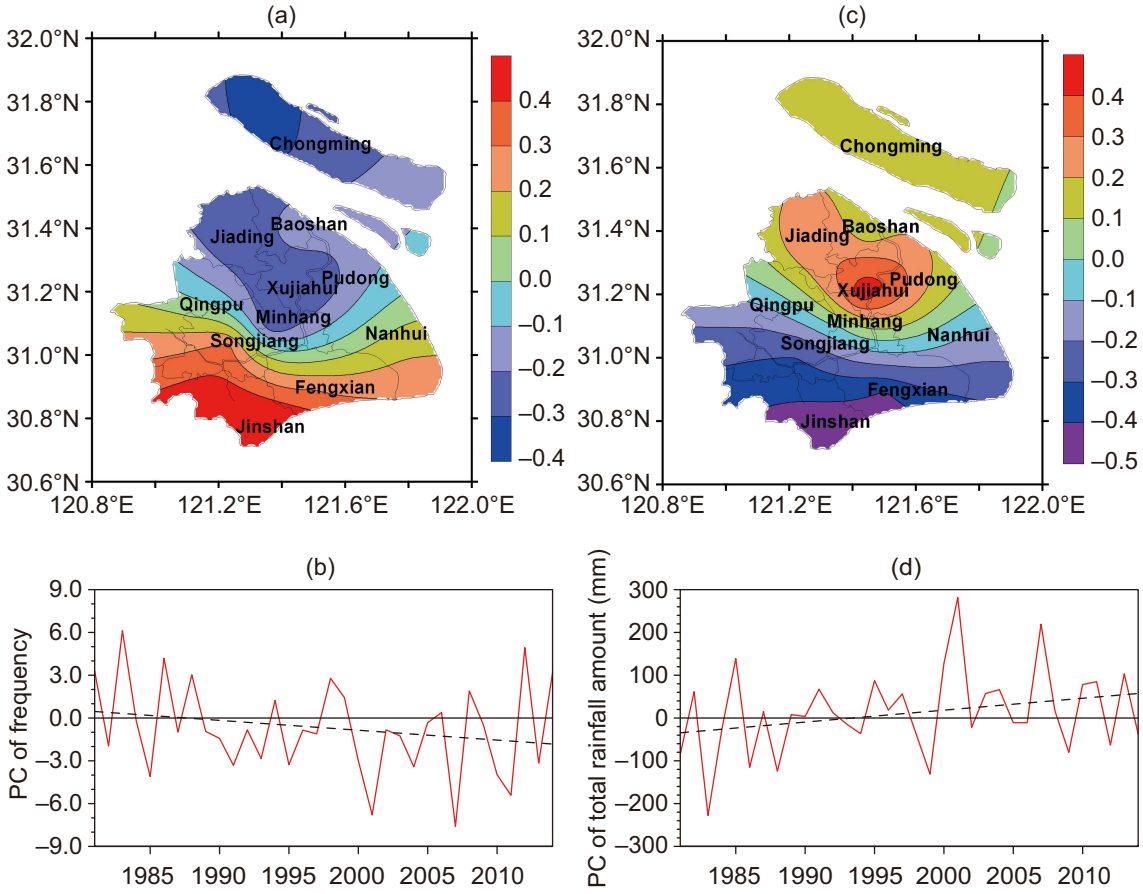

Fig. 6. Second EOF (a, c) eigenvectors and (b, d) principal components for the (a, b) frequency and (c, d) total rainfall amount (Unit: mm) of heavy rainfall events.

the impacts of urbanization on long-term changes in heavy precipitation, the percentage contribution of the urban rain-island effect (URIE) is defined as

$$\mathrm{URIE} = (\mathrm{TR}_{\mathrm{urban}} - \mathrm{TR}_{\mathrm{reg}})/\mathrm{TR}_{\mathrm{urban}} \times 100, \qquad (2)$$

where $\mathrm{TR}_{\mathrm{urban}}$ denotes the long-term trend of urban sites, and $\mathrm{TR}_{\mathrm{reg}}$ the regional average of the long-term trends for the whole of Shanghai. Thus, the contributions of the URIE on the long-term trends of total rainfall amount, frequency and intensity at urban sites are calculated according to Eq. (2).

Table 3 shows that the tendency of the total precipitation of heavy rainfall events at urban sites is 2.4 mm yr^{-1}, which is eight and two times greater than at rural (0.3 mm yr^{-1}) and suburban (1.2 mm yr^{-1}), respectively. For the whole of Shanghai on average, the tendency of the total heavy rainfall amount is 0.9 mm yr^{-1}. Therefore, based on Eq. (2), the contribution of urbanization to the long-term trend of the heavy rainfall amount at urban sites is as high as 62.5%. The contributions to the frequency and intensity of heavy precipitation at urban sites shows a similarly obvious urban–rural difference, i.e. the urban rain-island feature. Therein, the contribution to the increasing trend of the frequency of heavy rainfall reaches 54.7%, and the contrast between the trends for precipitation intensity at urban and rural sites is the most evident. Urban sites, such as Xujiahui and Pudong, increased significantly at the 95% and 90% confidence level, respectively; whereas, the increasing trend [0.3 mm h^{-1} $(10\ \mathrm{yr})^{-1}$] at suburban stations is less obvious, and rural stations show a weak declining trend. Thus, the contribution of urbanization to the trends of heavy rainfall intensity may be more than 50%, according to Eq. (2).

It can be seen from the above analysis that urbanization is conducive to enhancing both the occurrence and intensity of heavy rainfall events, thus further increasing the total amount of heavy precipitation. Urbanization may be responsible for more than half of the change trend at urban sites. The results, however, are mainly based on a linear tendency estimation method. To reduce the uncertainty of the above analysis,

Table 3. Comparison of the tendencies of hourly rainstorm events at different stations and the contributions of urban effects on trends at city sites.

Sites	Tendency of total precipitation (mm yr^{-1})	Tendency of frequency ($10\ \mathrm{yr}^{-1}$)	Tendency of intensity [mm h_{-1} $(10\ \mathrm{yr})^{-1}$]
Whole of Shanghai	0.9	0.29	0.19
Urban stations	2.4	0.64	2.3
Rural stations	0.3	0.16	−0.16
URIE (%)	62.5	54.7	> 50

considering rainfall as a nonlinear and nonstationary variable, the EEMD method was also applied to time series of the frequency, total rainfall amount and intensity of heavy precipitation events, to further investigate the urban–rural differences in the tendencies of heavy precipitation. By analyzing the trend components decomposed by EEMD, it was found that, compared with the linear tendency estimation method, the trends of total rainfall amount and frequency acquired by EEMD are more obvious, presenting even more distinct urbanization effects. For example, Fig. 7 shows a clearer urban–rural difference for the trends of heavy rainfall intensity during the rapid urbanization period after the end of the 1990s. In the 21st century, the intensity of urban heavy precipitation has increased year by year; whereas, at sites on the outskirts of the city, and in terms of the average for the whole of Shanghai, there has been little change. For the period 1981–2014, the intensity at urban sites enhanced from 29.8 mm h^{-1} in 1981 to 42.6 mm h^{-1} in 2014. Conversely, at sites on the outskirts of the city, or for the whole of Shanghai, growth was very slow. Thus, the EEMD analysis offers further support to the above results on the contribution of urbanization to the long-term change in heavy precipitation events.

5.3. *Influences on diurnal variation*

As shown in Fig. 8, the diurnal variation of rainfall intensity at both urban (Xujiahui and Pudong) and rural (Chongming, Nanhui, Jinshan, Qingpu, Fengxian) stations exhibits a unimodal-type trend, with the peak occurring during the afternoon to evening. Furthermore, the hourly precipitation at urban stations is much more intensive than that at rural sites during the peak hours (1600–2100 LST) of frequent heavy rainfall occurrence. The enhancement of precipitation in urban areas during the peak period is mainly realized by increased thermal and momentum transport. Heat is stored in urban materials during the daytime, and extra anthropogenic heat is then released to the urban boundary layer after late afternoon (Hu et al., 2016). Stronger turbulent vertical mixing and low-level water vapor convergence, due to both higher heat emissions and increased land surface roughness and surface friction velocity, in turn enhance the mean upward velocity and promote an increase in heavy precipitation in the afternoon to early evening over urban areas (Miao et al., 2011;

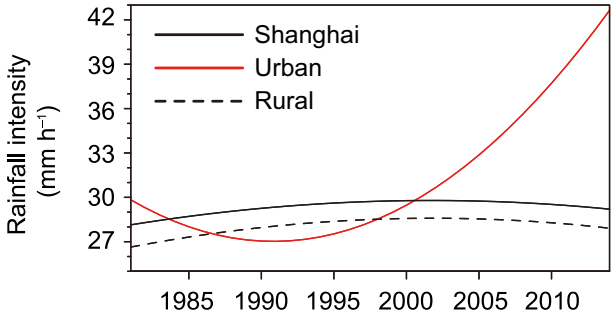

Fig. 7. Trends determined by EEMD applied to the intensities of heavy rainfall events during 1981–2014 (red line: urban area; black solid line: the whole of Shanghai; black dashed line: rural area).

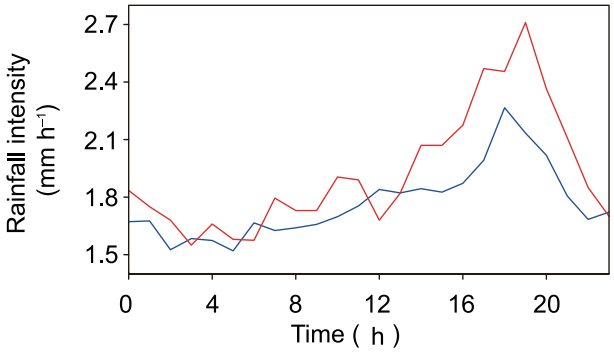

Fig. 8. Diurnal variation of hourly rainfall intensity at urban (red) and rural (blue) stations.

Hu et al., 2016; Song et al., 2016). At nighttime in Shanghai, when the urban heat island effect is most prominent, radiation cooling and the occurrence of sea breezes create conditions that are unfavorable to low-level upward motion and water vapor convergence. In other words, the most prominent urban rainfall island, during late afternoon to early evening, is mainly due to the combined influences of urban effects and basic local circulation associated with solar radiation and the sea breeze. The situation is similar for the enhancement of afternoon thunderstorms in Taipei (Chen et al., 2007). Moreover, the frequent occurrence period at urban sites (1600–2100 LST) is longer than that on the outskirts of the city (1700–2000). Furthermore, the peak time at city sites (1900 LST) is delayed by one hour compared with the outskirts of the city (1800 LST). Therefore, urbanization may lead to a greater occurrence of heavy precipitation and a delay in the peak rainfall time. These results are consistent with the modeling results of Ao et al. (2011) and Song et al. (2016).

6. Possible effects of climate change on the long-term variation of heavy precipitation

From the above analysis it is clear that the frequency of heavy precipitation increased significantly in Shanghai during the rapid urbanization period. Besides the urban–rural differences, the spatial distributions of the first EOF modes for the trends of the frequency and total precipitation amount for heavy rainfall events in Shanghai also show consistent variation. Next, we analyze and discuss the possible causes of these long-term tendencies from the viewpoint of climate change.

Following Seneviratne et al. (2016), who put forward a reasoning method for the regional responses to global climate forcing, we produce scatter plots (Fig. 9a) to show the scaling relationship between the changes in global mean temperature according to CRUTEM4 (Osborn and Jones, 2014) and the frequency anomaly of heavy rainfall events in Shanghai based on the decadal variation of the respective variables. The results indicate a rather linear scaling of heavy precipitation events in Shanghai with the global temperature anomaly, wherein their linear correlation passes the 0.01 reliability test. The frequency anomaly of regional heavy rainfall events in

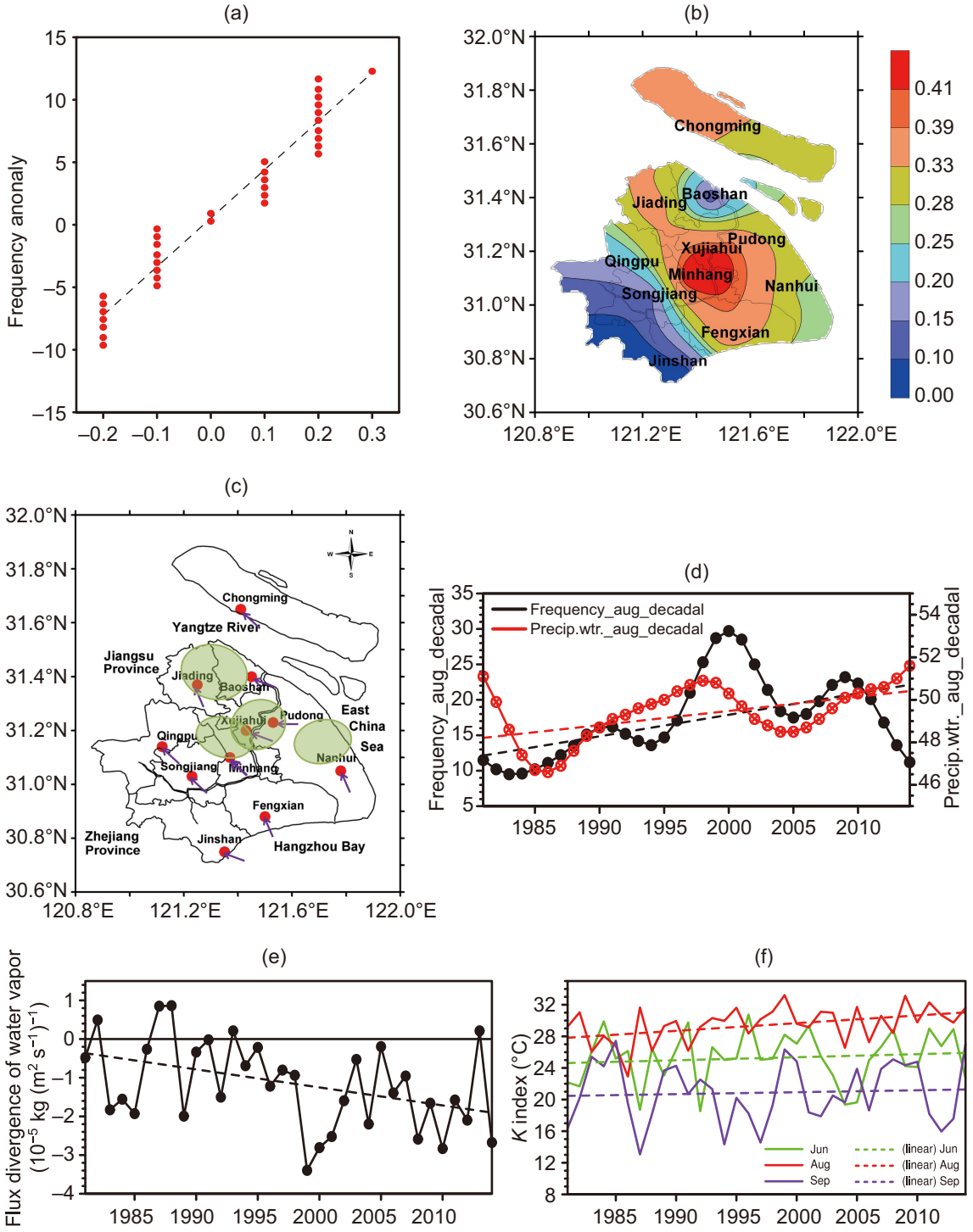

Fig. 9. Influential factors associated with the variation in hourly rainstorms over Shanghai during 1981–2014: (a) scaling between the anomaly percentage of hourly rainstorm frequency in Shanghai and the change in global mean temperature (*x*-axis denotes the temperature anomaly; units: °C; dashed line is the linear fitting line); (b) spatial distribution of correlation coefficients between 2-m air temperature and the frequency of hourly rainstorms during April–September; (c) prevailing wind directions in Shanghai during April–September (shaded areas denote distinct convergences of wind directions); (d) decadal variation (curve) and tendency (dashed line) for precipitable water (red; units: kg m^{-2}) and hourly rainstorm frequency (black) in August; (e) flux divergence of total-column water vapor transport over Shanghai during the summer half of the year [units: 10^{-5} kg $(m^2\ s^{-1})^{-1}$]; (f) *K* index (curve; units: °C) and tendency (dashed lines) over Shanghai in June, August and September.

Shanghai varies with the changes in global mean temperature. Relative to the average over 1981–2010, the frequency of heavy precipitation in Shanghai increases by 4% as the global mean temperature increases by 0.1°C. This indicates that surface warming is favorable to the occurrence of heavy rainfall events, which is consistent with the study of Trenberth (2005). Conversely, in terms of the spatial distribution of the correlation coefficients between temperature and the frequency of heavy rainfall events (Fig. 9b), high-correlation areas are located in the central city areas and nearby suburbs, especially in the city areas, with correlation coefficients passing the 0.05 reliability tests. Against the background of regionally consistent heating, the positive correlation between the occurrence of heavy precipitation and temperature is more significant over urban areas of Shanghai, where there is a prominent urban heat island effect (Zhou and Shu, 1994). In other words, the urban heat island contributes greatly to enhancing the occurrence of heavy rainfall events. At the same time, the high frequency over urban areas may be associated with the sea breeze circulation background. Figure 9c shows the prevailing wind directions in Shanghai during April to September. It can be seen that, as a coastal city, abundant moisture can be transported to Shanghai, with a prevalent southeasterly wind from its adjacent seas. In addition, the wind direction convergence zone over central city areas and nearby suburbs is rather similar to the heat-island area. This means that heavy precipitation events occur more easily under the presence of the heat island and sea breeze circulation. This is consistent with the results of Tan et al. (2015), who reported an example of short-duration convective precipitation falling over the northwestern part of Shanghai.

Surface warming also helps to raise atmospheric moisture. For example, in August, when the most pronounced increase in heavy precipitation occurs, the decadal variation of surface temperature is significantly and positively correlated with that of total-column precipitable water content. The correlation coefficient reaches 0.32 above the 95% confidence level. Furthermore, from Fig. 9d, the precipitable water content and frequency of heavy rainfall events in Shanghai during August show consistent decadal variations and long-term tendencies. Therefore, the increase in atmospheric moisture content associated with surface warming is another important cause of the enhancement in heavy rainfall events.

Water vapor convergence is a basic physical condition of precipitation. The long-term changes in the flux divergence of total-column water vapor transport over Shanghai during the summer half of the year are displayed in Fig. 9e. Water vapor convergence is dominant, with divergence showing a significant reducing trend. Specifically, the convergence of water vapor over Shanghai shows a significant (>99% confidence) increasing trend at a rate of 0.46×10^{-5} kg $(m^2\ s)^{-1}$. In addition, the average water vapor convergence during 1998–2014 is 1.75×10^{-5} kg $(m^2\ s)^{-1}$, which is almost three times more than that during the former period [1981–97; 0.61×10^{-5} kg $(m^2\ s)^{-1}$]. This provided a more favorable background for the occurrence of heavy precipitation.

Unstable atmospheric stratification is another important dynamic condition for the formation of heavy rainfall. The *K* index is adopted to explore the effects of atmospheric stability on the long-term change in heavy rainfall events. Figure 9f shows a significant (>99% confidence) increasing trend for the *K* index over Shanghai in August since 1981, with a rate of 1.0°C $(10\ yr)^{-1}$, indicating a significant enhancement in atmospheric instability. In addition, the average *K* index during the latter stage (1998–2014) reaches 30.4°C, which is favorable for the occurrence of strong convective weather and may thus be an important condition for the increase in heavy rainfall events. The situation in June is similar to that in August. Despite the weak increase of the *K* index in September [0.24° $(10\ yr)^{-1}$], the atmospheric stratification is not conducive to the occurrence of strong convective weather, owing to the low *K* index (<25°C) in most years. This is roughly consistent with the decreasing trend of heavy rainfall events in September. Furthermore, we also find that both surface temperature and the strength of the western Pacific subtropical high at 500 hPa are significantly correlated with the *K* index in August. This means that regional warming associated with large-scale circulation systems may contribute greatly to the increase in atmospheric instability, which is an important reason for the consistent increase in heavy rainfall events over the whole of Shanghai.

Combining the analyses in sections 5 and 6, it can be concluded that a background of increasing temperature, enhancing water vapor content, convergence of moisture flux and atmospheric instability, favorable for the formation of heavy precipitation, was responsible for the consistent increase in hourly heavy precipitation over the whole of Shanghai during the rapid urbanization period. Meanwhile, the urban rain-island effect contributed to more frequent and stronger heavy precipitation in central city areas, which is another important factor resulting in the long-term change in heavy precipitation frequency in the urban area. The preliminary estimation made in this study suggests that urbanization may account for more than half of the heavy precipitation tendencies at urban sites.

7. Conclusions

Based on hourly precipitation data in Shanghai covering a period of nearly a century (1916–2014), and from the perspective of extreme precipitation and the spatiotemporal distribution of hourly heavy rainfall events, the long-term variation in extreme heavy precipitation events in Shanghai were analyzed in this study, and the effects of urbanization and regional warming on heavy rainfall events investigated. The results can be summarized as follows.

Long-term annual variations of maximum hourly precipitation in Shanghai increased significantly during the last century, especially in the latter 50 years, with trends reaching 2.72 mm h^{-1} $(10\ yr)^{-1}$ and 6.2 mm h^{-1} $(10\ yr)^{-1}$ in the first and second half of the study period, respectively. In the latter half of the study period, the mean value of maximum precipitation intensity during the last 10 years (2005–

14; 85.5 mm h^{-1}) was about 1.5 times higher compared with that in the first 10 years (1965–74; 57 mm h^{-1}). The annual frequency of heavy hourly precipitation in Shanghai during the rapid urbanization period (1981–2014) showed a significant increasing trend, with more local and abrupt features. Specifically, the frequencies of local heavy rainfall events and abrupt heavy rainfall events increased at a rate of 1.5 and 1.8 $(10\ yr)^{-1}$, respectively—especially in June and August, when local or small-scale events mostly occur. The diurnal variation of the occurrence frequency of heavy precipitation exhibited a single-peak distribution type, with the peak occurring at 1700–2100 LST.

In terms of spatial distribution, the long-term trends for the frequency and total precipitation of hourly heavy rainfall exhibited clear city rain-island characteristics, with heavy precipitation events focused in urban and suburban areas. Urbanization was conducive to both an increase in frequency and an enhancement in intensity of heavy rainfall events at urban sites, thus further increasing the total precipitation of heavy rainfall events. In addition, urbanization also contributed to distinctive urban–rural differences in hourly rainfall intensity during the period from late afternoon to early evening, and further led to greater occurrences of heavy rainfall events near urban sites.

Regional warming, an enhancement of water vapor, moisture convergence and atmospheric instability provided favorable thermodynamic and dynamic conditions for the formation of extreme precipitation, which accounts for the consistent increase in hourly heavy precipitation over the whole of Shanghai during the rapid urbanization period. Moreover, from the correlation between 2-m air temperature and the frequency of strong rainfall events (Fig. 9b), there is some indication that the urban rain-island effects on heavy rainfall are linked with the interaction of the urban heat island, since frequencies of heavy rainfall are highly related with temperature in urban areas well-known as heat islands in Shanghai (Zhou and Shu, 1994). In addition, it was also found that the decreasing trend of the frequency of drizzle (<0.5 mm h^{-1}) was weaker over central city areas and the suburbs than on the outskirts during 1981–2014. Further analysis showed that drizzle frequencies over central city areas exhibited a slight increasing trend after 2007, while those over suburbs still decreased. This may be related with more warm cloud condensation nuclei coming from aerosols, which are advantageous to the formation of weak precipitation over central city areas (Zhou and Shu, 1994). The specific mechanism involved, however, needs further research.

It is important to note that the results of our analysis are limited in at least two respects. First, the spatial distribution of heavy precipitation in Shanghai was determined by 11 *in situ* meteorological stations that are sparsely distributed for interpolation purposes. Considering the local characteristics of heavy precipitation as depicted in this study, future analysis could be improved through the availability of additional high-resolution observations. And second, the use of simple correlation between temperature and precipitation at the 11 sites over Shanghai, to illustrate the impact of the urban heat island on heavy precipitation. Although further regression of the frequencies of heavy precipitation onto urban–rural temperature differences also showed the heat island effect may have led to the increase in heavy rainfall, the actual spatial distribution of the urban heat island may not take a fully concentric pattern (Hu et al., 2016) under the combined influences of both complex land-use categories and different weather conditions. Meanwhile, significant correlation between the frequencies of heavy rainfall were mainly found at those urban and suburban stations located in the downwind direction of the prevailing sea breeze. In other words, this significant correlation may be simultaneously associated with the impact of the sea breeze. Analysis of the relationship between heavy precipitation and the urban heat island could be further improved by excluding the impacts of the sea breeze through numerical modeling.

Acknowledgements. This research was jointly supported by the Major Consulting Projects of the Chinese Academy of Engineering ("Study on Strategies and Measures for the Prevention and Control of Urban Flood and Waterlogging Disasters in China"), the Public Welfare Industry (Meteorological) Research Projects (Grant Nos. GYHY201306065, GYHY201406001), and a research project of the Shanghai Meteorological Bureau (Grant No. YJ201604). The authors acknowledge the three anonymous reviewers, whose comments and suggestions helped to improve the paper.

REFERENCES

Alexandersson, H., 1986: A homogeneity test applied to precipitation data. *J. Climatol.*, **6**, 661–675.

Ao, X. Y., X. J. Ren, J. P. Tang, and X. Q. Yang, 2011: Simulation study of urbanization effects on summer daily precipitation over the Yangtze river delta. *Journal of the Meteorological Science*, **31**(4), 451–459. (in Chinese with English abstract)

Barnes, S. L., 1973: Mesoscale objective map analysis using weighted time series observations. NOAA Tech. Memo, ERL NSSL-62, 60 pp.

Boschat, G., A. Pezza, I. Simmonds, S. Perkins, T. Cowan, and A. Purich, 2015: Large scale and sub-regional connections in the lead up to summer heat wave and extreme rainfall events in eastern Australia. *Climate Dyn.*, **44**(7), 1823–1840.

Buishand, T. A. 1982: Some methods for testing the homogeneity of rainfall records. *J. Hydrol.*, **58**, 11–27.

Cai, M., Y. G. Ding, and Z. H. Jiang, 2007: Extreme precipitation experimentation over eastern china based on l-moment estimation. *Plateau Meteorology*, **26**(2), 309–318. (in Chinese with English abstract)

Chen, H. S., S. D. Fan, and X. H. Zhang, 2009: Seasonal differences of variation characteristics of extreme precipitation events over china in the last 50 years. *Transactions of Atmospheric Science*, **32**(6), 744–751. (in Chinese with English abstract)

Chen, T.-C., S.-Y. Wang, and M.-C. Yen, 2007: Enhancement of afternoon thunderstorm activity by urbanization in a valley: Taipei. *Journal of Applied Meteorology and Climatology*, **46**(9), 1324–1340.

Coles, S., J. Bawa, L. Trenner, and P. Dorazio, 2001: *An Introduction to Statistical Modeling of Extreme Values*. Springer,

London, 45–57.

Ding, Y. H., G. Y. Ren, Z. C. Zhao, Y. Xu, Y. Luo, Q. P. Li, and J. Zhang, 2007: Detection, causes and projection of climate change over China: An overview of recent progress. *Adv. Atmos. Sci.*, **24**(6), 954–971, doi: 10.1007/s00376-007-0954-4.

Ding, Y. H., Y. Sun, Z. Y. Wang, Y. X. Zhu, and Y. F. Song, 2009: Inter-decadal variation of the summer precipitation in China and its association with decreasing Asian summer monsoon Part II: Possible causes. *International Journal of Climatology*, **29**(13), 1926–1944.

Fu, G. B., N. R. Viney, S.P. Charles, and J. R. Liu, 2010: Long-term temporal variation of extreme rainfall events in Australia: 1910–2006. *Journal of Hydrometeorology*, **11**, 950–965.

Gao, X. Q., Tang L. C., and Zhu D. Q., 2004: Some thoughts on climate system and earth system. *Chinese Journal of Geophysics*, **47**(2), 364–368. (in Chinese with English abstract)

Grimm, A. M., and R. G. Tedeschi, 2009: ENSO and extreme rainfall events in South America. *J. Climate*, **22**(7), 1589–1609.

Han, Z. Q., Z. W. Yan, Z. Li, W. D. Liu, and Y. C. Wang, 2014: Impact of urbanization on low-temperature precipitation in Beijing during 1960–2008. *Adv. Atmos. Sci.*, **31**, 48–56, doi: 10.1007/s00376-013-2211-3.

Hao, L. P., Z. F. Fang, Z. L. Li, Z. Q. Liu, and J. H. He, 2007: The inter-annual climate change and heat island effect of Chengdu during the recent fifty years. *Scientia Meteorologica Sinica*, **27**, 648–654. (in Chinese with English abstract)

Hu, H. B., 2015: Spatiotemporal characteristics of rainstorm-induced hazards modified by urbanization in Beijing. *Journal of Applied Meteorology and Climatology*, **54**, 1496–1509.

Hu, X.-M., M. Xue, P. M. Klein, B. G. Illston, and S. Chen, 2016: Analysis of urban effects in Oklahoma City using a dense surface observing network. *Journal of Applied Meteorology and Climatology*, **55**(3), 723–741.

Hu, Y., and Q. Q. Li, 2010: The effects of solar wind system on atmospheric circulation in Shanghai. *The 27th Annual Meeting of China Meteorological Society City Weather, Better Life at the Venue*. (in Chinese)

Huang, A. N., Y. C. Zhang, and J. Zhu, 2009: Sensitivity of simulation of different intensity of summer precipitation over China to different cumulus convection parameterization schemes. *Chinese Journal of Atmospheric Sciences*, **33**, 1212–1224. (in Chinese with English abstract)

Huang, N. E., and Coauthors, 1998: The empirical mode decomposition and the Hilbert spectrum for nonlinear and non-stationary time series analysis. *Proc. R. Soc.* London, **454**(1971), 903–995.

Huang, W., R. C. Yu, and J. Li, 2012: Analysis of changes in precipitation intensity in later-summer over southeast coast of China in 1967–2006. *Progressus Inquisitiones de Mutatione Climatis*, **8**, 164–170. (in Chinese with English abstract)

IPCC, 1990: *Climate Change: The IPCC Scientific Assessment*. Report prepared for Intergovernmental Panel on Climate Change by Working Group I, J. T. Houghton et al., Eds., Cambridge University Press, 1–365.

IPCC, 2013: *Climate Change 2013: The Physical Science Basis*. Contribution of Working Group I to the Fifth Assessment Report of the Intergovernmental Panel on Climate Change, Stocker et al., Eds., Cambridge University Press, doi: 10.1017/CBO9781107415324, 1535 pp.

Kalnay, E., and Coauthors, 1996: The NCEP/NCAR 40-year reanalysis project. *Bull. Amer. Meteor. Soc.*, **77**, 437–471.

Kendall, M. G., 1975: *Rank Correlation Methods*. Griffin & Co, London.

Li, J., R. C. Yu, and W. Sun, 2013: Duration and seasonality of the hourly extreme rainfall in the central-eastern part of China. *Acta Meteorologica Sinica*, **71**, 652–659. (in Chinese with English abstract)

Liang, P., Y. H. Ding, J. H. He, and X. Tang, 2013: Study of relationship between urbanization speed and change in spatial distribution of rainfall over Shanghai. *Journal of Tropical Meteorology*, **19**, 97–103.

Lin, J., and G. M. Yang, 2014: Spatial-temporal characteristics of rainstorm in China during 1981–2010. *Meteorological Monthly*, **40**, 816–826. (in Chinese with English abstract)

Liu, R., S. C. Liu, C. J. Shiu, J. Li, and Y. H. Zhang, 2016: Trends of regional precipitation and their control mechanisms during 1979–2013. *Adv. Atmos. Sci.*, **33**, 164—174, doi: 10.1007/s00376-015-5117-4.

Liu, X. F., L. Xiang, and C. W. Yu, 2010: Characteristics of temporal and spatial variations of the precipitation extremes in the Haihe River Basin. *Climatic and Environmental Research*, **15**, 451–461. (in Chinese with English abstract)

Lorenz, E. N., 1956: Empirical orthogonal functions and statistical weather prediction. *Sci. Rep.*, **409**, 997–999.

Mann, H. B., 1945: Nonparametric tests against trend. *Econometrica*, **13**, 245–259.

Meals, D. W., J. Spooner, S. A. Dressing, and J. B. Harcum, 2011: Statistical analysis for monotonic trends. Tech Notes, No. 6, 23.

Miao, S. G., F. Chen, Q. C. Li, and S. Y. Fan, 2011: Impacts of urban processes and urbanization on summer precipitation: a case study of heavy rainfall in Beijing on 1 August 2006. *Journal of Applied Meteorology and Climatology*, **50**(4), 806–825.

Mu, H. Z., C. Y. Kong, X. Tang, and X. X. Ke, 2008: Preliminary analysis of temperature change in Shanghai and urbanization impacts. *Journal of Tropical Meteorology*, **24**, 672–678. (in Chinese with English abstract)

Osborn, T. J., and P. D. Jones, 2014: The CRUTEM4 land-surface air temperature data set: construction, previous versions and dissemination via google earth. *Earth System Science Data*, **6**, 61–68.

Pattanaik, D. R., and M. Rajeevan, 2010: Variability of extreme rainfall events over India during southwest monsoon season. *Meteorological Applications*, **17**(1), 88–104.

Pettitt, A. N., 1979: A non-parametric approach to the change-point problem. *Applied Statistics*, **28**, 126–135.

Piao, S. L., and Coauthors, 2010: The impacts of climate change on water resources and agriculture in China. *Nature*, **467**, 43–51.

Seneviratne, S. I., M. G. Donat, A. J. Pitman, R. Knutti, and R. L. Wilby, 2016: Allowable CO_2 emissions based on regional and impact-related climate targets. *Nature*, **529**, 477–483.

Song, Y. Q., H. N. Liu, X. Y. Wang, N. Zhang, and J. N. Sun, 2016: Numerical simulation of the impact of urban non-uniformity on precipitation. *Adv. Atmos. Sci.*, **33**(6), 783–793, doi: 10.1007/s00376-016-5042-1.

Sun, J. S., and W. J. Shu, 2007: The effect of urban heat island on winter and summer precipitation in Beijing region. *Chinese Journal of Atmospheric Sciences*, **31**, 311–320. (in Chinese with English abstract)

Tan, J. G., and Coauthors, 2015: Urban integrated meteorological observations: Practice and experience in Shanghai, China.

Bull. *Amer*. *Meteor*. *Soc*., **96**, 85–102.

Trenberth, K., 2005: Uncertainty in hurricanes and global warming. *Science*, **308**, 1753–1754.

Vicente-Serrano, S. M., S. Beguería, J. I. López-Moreno, A. M. El Kenawy, and M. Angulo-Martínez, 2009: Daily atmospheric circulation events and extreme precipitation risk in northeast Spain: Role of the north Atlantic oscillation, the western Mediterranean oscillation, and the Mediterranean oscillation. *J*. *Geophys*. *Res*., **114**, D08106.

Wang, X. M., X. D. Yu and Z. He, 2012: The applicability of NCEP Reanalysis data to severe convection environment analysis. *Journal of Applied Meteorological Science*, **23**(2), 139–146. (in Chinese)

Wang, X. Q., Z. F. Wang, Y. B. Qi, and H. Guo, 2009: Effect of urbanization on the winter precipitation distribution in Beijing area. *Science in China Series D: Earth Sciences*, **52**, 250–256.

Wei, F. Y., 2007: *Modern climatic Statistical Diagnosis and Prediction Technology*. China Meteorological Press, 37–41. (in Chinese)

Wijngaard J. B., A. M. G. K. Tank, and G. P. Können, 2003: Homogeneity of 20th century European daily temperature and precipitation series. *International Journal of Climatology*, **23**(6), 679–692.

Wu, Z. H., and N. E. Huang, 2005: Ensemble empirical mode decomposition: a noise-assisted data analysis method. COLA Tech. Rep, No. 193, Center for Ocean–Land–Atmosphere Studies, Calverton, Maryland.

Wu, Z. H., and N. E. Huang, 2009: Ensemble empirical mode decomposition: A noise-assisted data analysis method. *Advances in Adaptive Data Analysis*, **1**, 1–41, doi: 10.1142/S1793536909000047.

Xu, Y. M., 2006: *China Meteorological Disasters Dictionary* (*Shanghai Volume*). Meteorological Press, Beijing, 222 pp. (in Chinese)

Yin, S. Q., G. Gao, W. Jing, D. L. Chen, and L. S. Hao, 2011a: Long-term precipitation change by hourly data in Haihe River Basin during 1961–2004. *Science China D: Earth Sciences*, **54**, 1576–1585.

Yin, S. Q., W. J. Li, D. L. Chen, J. H. Jeong, and W. L. Guo, 2011b: Diurnal variations of summer precipitation in the Beijing area and the possible effect of topography and urbanization. *Adv. Atmos. Sci*., **28**(4), 725–734, doi: 10.1007/s00376-010-9240-y.

Yu, H., G. Y. Yang, Z. H. Zhou, J. H. Wang, and D. Y. Qin, 2008: Variation of summer precipitation in Tianjin region and its urbanization effect. *Progress in Geography*, **27**(5), 43–48. (in Chinese with English abstract)

Yu, R. C., J. Li, H. M. Chen, and W. H. Yuan, 2014: Progress in studies of the precipitation diurnal variation over contiguous China. *Meteorological Bulletin*, **72**(5), 948–968. (in Chinese with English abstract)

Zhai, P. M., C. C. Wang, and W. Li, 2007: A review on study of change in precipitation extremes. *Advances in Climate Change Research*, **3**(3), 144–148. (in Chinese with English abstract)

Zhang, G. C., and Coauthors, 2007: *Techniques and Methods of Contemporary Weather Forecast*. China Meteorological Press, Beijing, 117 pp. (in Chinese)

Zhang, H., and P. M. Zhai, 2011: Temporal and spatial characteristics of extreme hourly precipitation over eastern China in the warm season. *Adv. Atmos. Sci*., **28**, 1177–1183, doi: 10.1007/s00376-011-0020-0.

Zhou, J. K., H. H. Huang, Y. Y. Tang, and H. G. Zhu, 2003: Influence of urbanization on regional precipitation of Nanjing City. *Journal of Yangtze River Scientific Research Institute*, **20**(4), 44–46. (in Chinese with English abstract)

Zhou, L. Y., and K. Yang, 2001: Variation of precipitation in Shanghai during the last one hundred years and precipitation differences between city and suburb. *Acta Geographica Sinica*, **56**(4), 467–476. (in Chinese with English abstract)

Zhou, S. Z., and J. Shu, 1994: *Urban Climatology*. China Meteorological Press, Beijing. (in Chinese)

Zhou, Y. X., and Y. L. Shi, 1995: Toward establishing the concept of physical urban area in China. *Acta Geographica Sinica*, **50**(4), 289–301. (in Chinese with English abstract)